7. S. Kirkpatrick, B. Selman, *Science* **264**, 1297 (1994).
8. E. Farhi *et al.*, unpublished data.
9. L. K. Grover, *Phys. Rev. Lett.* **78**, 325 (1997).
10. E. Farhi, S. Gutmann, *Phys. Rev. A* **57**, 2403 (1998); C. H. Bennett, E. Bernstein, G. Brassard, U. V. Vazirani, *SIAM J. Comput.* **26**, 1510 (1997) (available at http://xxx.lanl.gov/abs/quant-ph/9701001).
11. A. M. Childs, E. Farhi, J. Goldstone, S. Gutmann, http://xxx.lanl.gov/abs/quant-ph/0012104.
12. Supported in part by the U.S. Department of Energy under cooperative agreement DE-FC02-94ER40818 and also by MIT's Undergraduate Research Opportunities Program. We thank the Computer Facility of the MIT Laboratory for Nuclear Science for extensive use of the computer Abacus. We benefited greatly from conversations with A. Childs, B. Selman, and L. Valiant. We also thank D. Fisher, B. Halperin, M. Kardar, and P. Lee for useful discussions about the connection of our work to statistical mechanics systems.

27 November 2000; accepted 19 March 2001

# Observation of Vortex Lattices in Bose-Einstein Condensates

**J. R. Abo-Shaeer, C. Raman, J. M. Vogels, W. Ketterle**

**Quantized vortices play a key role in superfluidity and superconductivity. We have observed the formation of highly ordered vortex lattices in a rotating Bose-condensed gas. These triangular lattices contained over 100 vortices with lifetimes of several seconds. Individual vortices persisted up to 40 seconds. The lattices could be generated over a wide range of rotation frequencies and trap geometries, shedding light on the formation process. Our observation of dislocations, irregular structure, and dynamics indicates that gaseous Bose-Einstein condensates may be a model system for the study of vortex matter.**

The quantization of circulation has a profound effect on the behavior of macroscopic quantum systems. Magnetic fields can penetrate type-II superconductors only as quantized flux lines. Vorticity can enter rotating superfluids only in the form of discrete line defects with quantized circulation. These phenomena are direct consequences of the existence of a macroscopic wavefunction, the phase of which must change by integer multiples of $2\pi$ around magnetic flux or vortex lines. In superconductors, magnetic flux lines arrange themselves in regular lattices that have been directly imaged (*1*). In superfluids, direct observation of vortices has been limited to small arrays (up to 11 vortices), both in liquid $^4$He (*2*) and, more recently, in rotating gaseous Bose-Einstein condensates (BECs) (*3*, *4*).

We report the observation of vortex lattices in a BEC. We are now able to explore the properties of bulk vortex matter, which includes local structure, defects, and long-range order. In contrast, the properties of small arrays are strongly affected by surface and finite size effects. The vortex lattices are highly excited collective states of BECs with an angular momentum of up to 60 $\hbar$ per particle. Our experiments show that such states can be prepared and are much more stable than predicted (*5*).

Vortices in BECs have been the subject of extensive theoretical study (*6*). Experimental progress began only recently with the observation of quantized circulation in a two-component condensate by a phase engineering technique (*7*) and of vortex arrays in a single-component BEC (*3*). A condensate can be subjected to a rotating perturbation by revolving laser beams around it. This technique was used to study surface waves in a trapped BEC (*8*), and subsequently for the creation of vortices (*3*). In 1997, we tried unsuccessfully to detect quantized circulation as a "centrifugal hole" in ballistic expansion of the gas (*9*, *10*). Theoretical calculations (*11–13*) and ultimately the pioneering experimental work (*3*) showed that vortices can indeed be detected through ballistic expansion, which magnifies the spatial structure of the trapped condensate.

BECs of up to $5 \times 10^7$ Na atoms with a negligible thermal component (condensate fraction $\geq$ 90%) were produced by a combination of laser and evaporative cooling techniques (*8*, *10*, *14*). A radio-frequency "shield" limited the magnetic trap depth to 50 kHz (2.3 $\mu$K), preventing high-energy atoms from heating the condensate. Experiments were performed in cylindrical traps with widely varying aspect ratios. Most of the results and all of the images were obtained in a weak trap, with radial and axial frequencies of $\nu_r = 84$ Hz and $\nu_z = 20$ Hz (aspect ratio 4.2), respectively. In this weak trap inelastic losses were suppressed, resulting in larger condensates of typically $5 \times 10^7$ atoms. Such clouds had a chemical potential ($\mu$) of 310 nK (determined from time-of-flight imaging), a peak density of $4.3 \times 10^{14}$ cm$^{-3}$, a Thomas-Fermi radius along the radial direction ($R_r$) of 29 $\mu$m, and a healing length ($\xi$) of about 0.2 $\mu$m.

Vortex lattices were produced by rotating the condensate around its long axis with the optical dipole force exerted by blue-detuned laser beams at a wavelength of 532 nm. A two-axis acousto-optic deflector generated a pattern of two laser beams rotating symmetrically around the condensate at variable drive frequency $\Omega$ (*8*). The two beams were separated by one Gaussian beam waist ($w$ = 25 $\mu$m). The laser power of 0.7 mW in each beam corresponded to an optical dipole potential of 115 nK. This yielded a strong, anharmonic deformation of the condensate.

After the condensate was produced, the stirring beam power was ramped up over 20 ms, held constant for a variable stirring time, and then ramped down to zero over 20 ms. The condensate equilibrated in the magnetic trap for a variable hold time (typically 500 ms). The trap was then suddenly switched off, and the gas expanded for 35 ms to radial and axial sizes of $l_r \cong 1000$ $\mu$m and $l_z \cong 600$ $\mu$m, respectively. We probed the vortex cores using resonant absorption imaging. To avoid blurring of the images due to bending of the cores near the edges of the condensate, we pumped a thin, 50- to 100-$\mu$m slice of atoms in the center of the cloud from the $F = 1$ to the $F = 2$ hyperfine state (*15*). This section was then imaged along the axis of rotation with a probe pulse resonant with the cycling $F = 2 \rightarrow 3$ transition. The duration of the pump and probe pulses was chosen to be sufficiently short (50 and 5 $\mu$s, respectively) to avoid blurring due to the recoil-induced motion and free fall of the condensate.

We observed highly ordered triangular lattices of variable vortex density containing up to 130 vortices (Fig. 1). A striking feature is the extreme regularity of these lattices, free of any major distortions, even near the boundary. Such "Abrikosov" lattices were first predicted for quantized magnetic flux lines in type-II superconductors (*16*). Tkachenko showed that their lowest energy structure should be triangular for an infinite system (*17*). A slice through images shows the high visibility of the vortex cores (Fig. 2), which was as high as 80%. For a trapped condensate with maximum vortex density, we infer that the distance between the vortices was $\cong$ 5 $\mu$m. The radial size of the condensate in the time-of-flight images was over 10% larger when it was filled with the maximum number of vortices, probably due to centrifugal forces.

When a quantum fluid is rotated at a frequency $\Omega$, it attempts to distribute the vorticity as uniformly as possible. This is similar to a rigid body, for which the vorticity

Department of Physics, Center for Ultracold Atoms at Massachusetts Institute of Technology (MIT) and Harvard University, and Research Laboratory of Electronics, MIT, Cambridge, MA 02139, USA.

*To whom correspondence should be addressed. E-mail: jamil@mit.edu

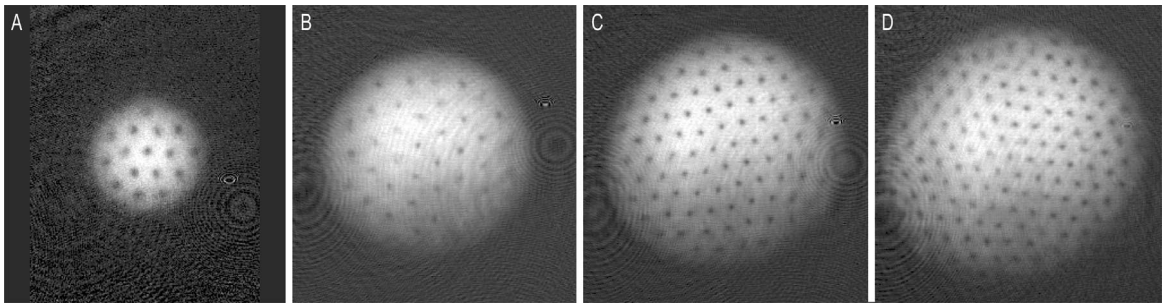


**Fig. 1.** Observation of vortex lattices. The examples shown contain approximately (**A**) 16, (**B**) 32, (**C**) 80, and (**D**) 130 vortices. The vortices have "crystallized" in a triangular pattern. The diameter of the cloud in (D) was 1 mm after ballistic expansion, which represents a magnification of 20. Slight asymmetries in the density distribution were due to absorption of the optical pumping light.

is constant $\nabla \times \vec{\mathbf{v}} = 2\vec{\Omega}$. For a superfluid, the circulation of the velocity field, $\vec{\mathbf{v}}$, is quantized in units of $\kappa = h/M$, where $M$ is the atomic mass and $h$ is Planck's constant. The quantized vortex lines are distributed in the fluid with a uniform area density (*18*)

$$n_v = 2\Omega/\kappa \quad (1)$$

In this way the quantum fluid achieves the same average vorticity as a rigidly rotating body, when "coarse-grained" over several vortex lines. For a uniform density of vortices, the angular momentum per particle is $N_v\hbar/2$, where $N_v$ is the number of vortices in the system.

The number of observed vortices is plotted as a function of stirring frequency $\Omega$ for two different stirring times (Fig. 3). The peak near 60 Hz corresponds to the frequency $\Omega/2\pi = \nu_r/\sqrt{2}$, where the asymmetry in the trapping potential induced a quadrupolar surface excitation, with angular momentum $l = 2$, about the axial direction of the condensate (the actual excitation frequency of the surface mode $\nu = \sqrt{2}\nu_r$ is two times larger due to the twofold symmetry of the quadrupole pattern). The same resonant enhancement in the vortex production was observed for a stiff trap, with $\nu_r = 298$ Hz and $\nu_z = 26$ Hz (aspect ratio 11.5), and has recently been studied in great detail for small vortex arrays (*19*).

Far from the resonance, the number of vortices produced increased with the stirring time. By increasing the stir time up to 1 s, vortices were observed for frequencies as low as 23 Hz ($\cong 0.27\nu_r$). Similarly, in a stiff trap we observed vortices down to 85 Hz ($\cong 0.29\ \nu_r$). From Eq. 1 one can estimate the equilibrium number of vortices at a given rotation frequency to be $N_v = 2\pi R^2\Omega/\kappa$. The observed number was always smaller than this estimate, except near resonance. Therefore, the condensate did not receive sufficient angular momentum to reach the ground state in the rotating frame. In addition, because the drive increased the moment of inertia of the condensate (by weakening the trapping potential), we expect the lattice to rotate faster after the drive is turned off.

Looking at time evolution of a vortex lattice (Fig. 4), the condensate was driven near the quadrupole resonance for 400 ms and then probed after different periods of equilibration in the magnetic trap. A blurry structure was already visible at early times. Regions of low column density are probably vortex filaments that were misaligned with the axis of rotation and showed no ordering (Fig. 4A). As the dwell time increased, the filaments began to disentangle and align with the axis of the trap (Fig. 4, B and C), and finally formed a completely ordered Abrikosov lattice after 500 ms (Fig. 4D). Lattices with fewer vortices could be generated by rotating the condensate off resonance. In these cases, it took longer for regular lattices to form. Possible explanations for this observation are the weaker interaction between vortices at lower vortex density and the larger distance they must travel to reach their lattice sites. In principle, vortex lattices should have already formed in the rotating, anisotropic trap. We suspect that intensity fluctuations of the stirrer or improper beam alignment prevented this.

The vortex lattice had lifetimes of several seconds (Fig. 4, E to G). The observed stability of vortex arrays in such large condensates is surprising because in previous work the lifetime of vortices markedly decreased with the number of condensed atoms (*3*). Theoretical calculations predict a lifetime inversely proportional to the number of vortices (*5*). Assuming a temperature $k_BT \cong \mu$, where $k_B$ is the Boltzmann constant, the predicted decay time of $\cong$ 100 ms is much shorter than observed. After 10 s, the number of vortices

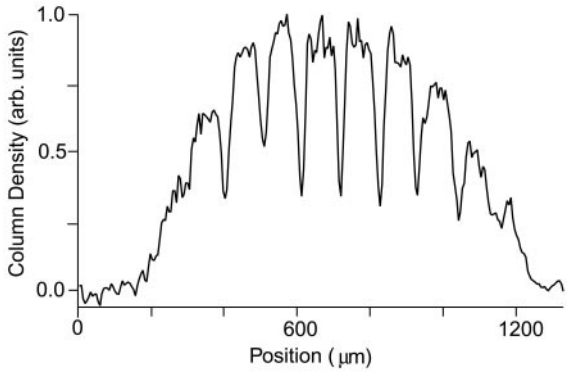


**Fig. 2.** Density profile through a vortex lattice. The curve represents a 5-μm-wide cut through a two-dimensional image similar to those in Fig. 1 and shows the high contrast in the observation of the vortex cores. The peak absorption in this image is 90%.

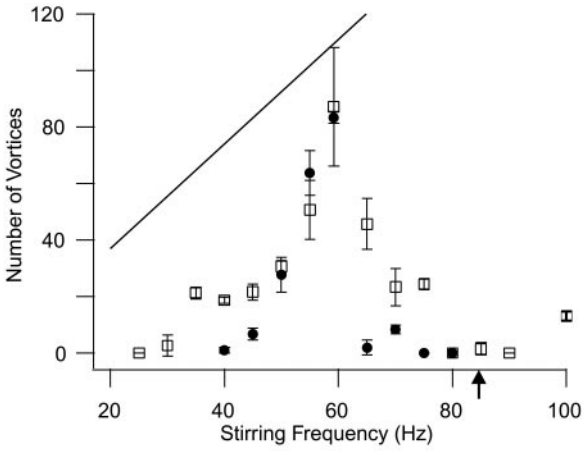


**Fig. 3.** Average number of vortices as a function of the stirring frequency $\Omega$ for two different stirring times, (●) 100 ms and (□) 500 ms. Each point represents the average of three measurements with the error bars given by the standard deviation. The solid line indicates the equilibrium number of vortices in a radially symmetric condensate of radius $R_r = 29$ μm, rotating at the stirring frequency. The arrow indicates the radial trapping frequency.

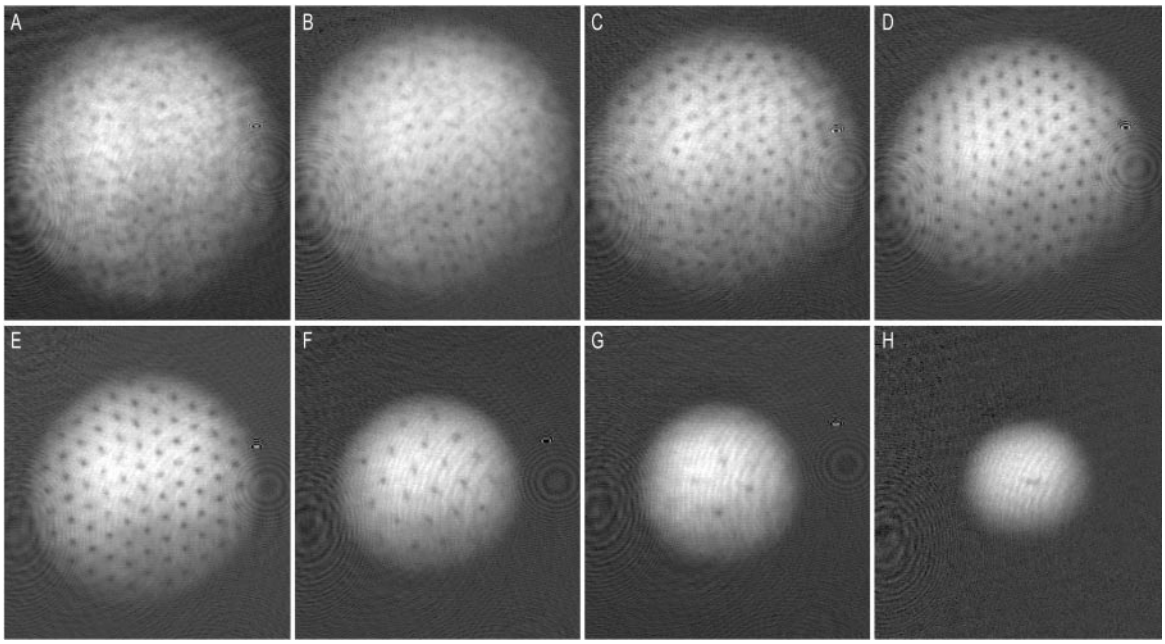


**Fig. 4.** Formation and decay of a vortex lattice. The condensate was rotated for 400 ms and then equilibrated in the stationary magnetic trap for various hold times. (**A**) 25 ms, (**B**) 100 ms, (**C**) 200 ms, (**D**) 500 ms, (**E**) 1 s, (**F**) 5 s, (**G**) 10 s, and (**H**) 40 s. The decreasing size of the cloud in (E) to (H) reflects a decrease in atom number due to inelastic collisions. The field of view is ~1 mm by 1.15 mm.

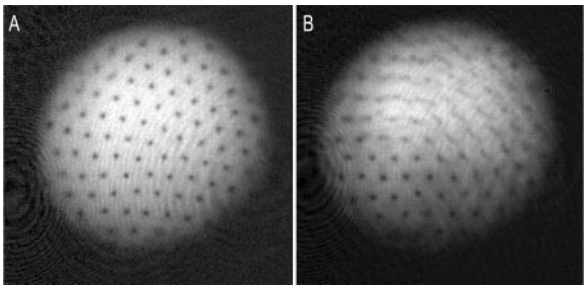


**Fig. 5.** Vortex lattices with defects. In (**A**), the lattice has a dislocation near the center of the condensate. In (**B**), there is a defect reminiscent of a grain boundary.

had diminished considerably. In several cases we observed a single vortex near the condensate center after 30 to 40 s (Fig. 4H). This dwell time is much longer than that observed for elongated clouds (1 to 2 s) (*3*) and for nearly spherical condensates (15 s) (*20*). We estimate that during its lifetime, the superfluid flow field near the central vortex core had completed more than 500,000 revolutions and the lattice itself had rotated ~100 times.

A feature of the lattices is their almost perfect triangular shape. Deformations are less pronounced than in theoretical calculations that predicted circular distortions (*13*, *21*). It was shown (*21*) that a configuration with perfect triangular symmetry can lower its energy by rearranging the outermost ring of vortices into a circle. This distortion is caused by the cylindrical symmetry of rotation and not by boundary effects (which were neglected in the calculations). In condensates of finite size and inhomogeneous density, one may expect even larger distortions. However, in images containing large numbers of vortices (Fig. 1, C and D), the lattice is triangular throughout the condensate even up to the edge. We have observed more complex lattice configurations in a fraction of the images. Some show patterns characteristic of partial crystallization (Fig. 4B), dislocations (Fig. 5A), and grain boundaries (Fig. 5B).

Our experiments may shed light on the ongoing discussion of vortex formation (*6*). A single vortex is expected to be thermodynamically stable when the rotation frequency exceeds (*22*)

$$\Omega_C = \frac{5}{2}\frac{\hbar}{MR_r^2}\ln\left[\frac{0.671R_r}{\zeta}\right] \qquad (2)$$

For our trap this yields a critical angular frequency of $\cong 2\pi \times 6$ Hz, or $0.08\omega_r$. Vortices were only observed at rotation frequencies much higher than $\Omega_C$. Some have suggested that the critical frequency of $\cong 0.7\ \omega_r$ observed in other experiments was related to the suppression of unstable excitations (so-called anomalous modes) of rectilinear vortices (*6*, *23*, *24*). These anomalous modes depend strongly on the aspect ratio of the trap. Our observation of vortices at $\sim 0.25\omega_r$ in traps where the aspect ratio varied by a factor of 2.7 seems to rule out a crucial role of the anomalous modes, possibly because their frequencies are lower for dense condensates.

Apart from stability conditions, vortices must be nucleated. Several theoretical papers have discussed the barrier for the entry of a vortex from the edge (*6*, *25*, *26*). The condensate becomes unstable against surface deformations when the stirring frequency exceeds

$$\Omega_s = \min_l(\omega_l/l) \qquad (3)$$

where $\omega_l$ is the frequency of a surface excitation with angular momentum $l$ in the axisymmetric trap (*27*, *28*). For our condensates, the instability is predicted to occur at $l \cong 18$, yielding $\Omega_s \cong 0.3\omega_r$, which is in fair agreement with our observations (*29*). The instabilities occur on a practical time scale only when the cloud is sufficiently deformed to excite high-$l$ modes. In other experiments (*3*, *19*), a sizable deformation was achieved only by resonantly driving the $l = 2$ mode near $0.7\omega_r$. In contrast, we strongly deformed the condensate over a broad range of frequencies. For such deformations, $l$ is no longer a good quantum number, allowing for coupling into higher-order modes. Our technique is therefore well suited to studying the threshold for vortex formation.

The surface instability criterion of Eq. 3 applies to rotational excitation. In the spirit of our earlier stirring experiments on critical velocities (*14*, *30*), we also explored linear motion of the stirrer. When we moved a small laser beam ($\cong 10$ μm in diameter) at a velocity of 2 mm/s once through the condensate along the radial direction, we observed large lattices containing $\cong 50$ vortices after an equilibration time of 1 s, indistinguishable from those generated with the rotating anisotropy. We assume that imperfect alignment of the stirring beam imparted a torque on the condensate. However, the mechanism of vortex formation warrants further study.

Properties of vortex lattices are of broad interest in superfluids, superconductors, and even astrophysics. Fluctuations in the rotation rate of pulsars are attributed to the dynamics of the vortex lattice in a superfluid neutron liquid (*5*, *31*). Our experiments show that vortex formation and self-assembly into a regular lattice is a robust feature of rotating BECs. Gaseous condensates may serve as a model system to study the dynamics of vortex matter, in analogy to work in type-II superconductors (*32*). Of particular interest are collective modes of the lattice. In liquid helium, transverse oscillations in a vortex lattice (Tkachenko oscillations) have already been investigated (*33*, *34*). Further studies may address the nucleation, ordering, and decay of lattices, in particular to delineate the role of the thermal component (*5*), and possible phase transition associated with melting and crystallization.

**References and Notes**


1. H. Träuble, U. Essmann, *Phys. Lett.* **24A**, 526 (1967).
2. E. J. Yarmchuk, M. J. V. Gordon, R. E. Packard, *Phys. Rev. Lett.* **43**, 214 (1979).
3. K. W. Madison, F. Chevy, W. Wohlleben, J. Dalibard, *Phys. Rev. Lett.* **84**, 806 (2000).
4. _____, *J. Mod. Opt.* **47**, 2715 (2000).
5. P. O. Fedichev, A. E. Muryshev, preprint available at http://arXiv.org/abs/cond-mat/0004264.
6. Reviewed in A. L. Fetter, A. A. Svidzinsky, *J. Phys. Condens. Matter* **13**, R135 (2001).
7. M. R. Matthews *et al.*, *Phys. Rev. Lett.* **83**, 2498 (1999).
8. R. Onofrio *et al.*, *Phys. Rev. Lett.* **84**, 810 (2000).
9. M. R. Andrews, thesis, Massachusetts Institute of Technology (1998).
10. Reviewed in W. Ketterle, D. S. Durfee, D. M. Stamper-Kurn, in *Bose-Einstein Condensation in Atomic Gases*, *Proceedings of the International School of Physics Enrico Fermi, Course CXL*, M. Inguscio, S. Stringari, C. Wieman, Eds. (International Organisations Services B.V, Amsterdam, 1999), pp. 67–176.
11. E. Lundh, C. J. Pethick, H. Smith, *Phys. Rev. A* **58**, 4816 (1998).
12. F. Dalfovo, M. Modugno, *Phys. Rev. A* **61**, 023605 (2000).
13. Y. Castin, R. Dum, *Eur. Phys. J. D* **7**, 399 (1999).
14. R. Onofrio *et al.*, *Phys. Rev. Lett.* **85**, 2228 (2000).
15. M. R. Andrews *et al.*, *Science* **275**, 637 (1997).
16. A. A. Abrikosov, *J. Exp. Theor. Phys.* **5**, 1174 (1957) [*Zh. Eksp. Teor. Fiz.* **32**, 1442 (1957)].
17. V. K. Tkachenko, *J. Exp. Theor. Phys.* **22**, 1282 (1966) [*Zh. Eksp. Teor. Fiz.* **49**, 1875 (1965)].
18. P. Nozières, D. Pines, *The Theory of Quantum Liquids* (Addison-Wesley, Redwood City, CA, 1990).
19. K. W. Madison, F. Chevy, V. Bretin, J. Dalibard, preprint available at http://arXiv.org/abs/cond-mat/?0101051.
20. P. C. Haljan, B. P. Anderson, I. Coddington, E. A. Cornell, preprint available at http://arXiv.org/abs/cond-mat/0012320.
21. L. J. Campbell, R. M. Ziff, *Phys. Rev. B* **20**, 1886 (1979).
22. E. Lundh, C. J. Pethick, H. Smith, *Phys. Rev. A* **55**, 2126 (1997).
23. D. L. Feder, A. A. Svidzinsky, A. L. Fetter, C. W. Clark, *Phys. Rev. Lett.* **86**, 564 (2001).
24. J. J. García-Ripoll, V. M. Pérez-García, preprint available at http://arXiv.org/abs/cond-mat/0012071; _____, preprint available at http://arXiv.org/abs/con-mat/0101219.
25. T. Isoshima, K. Machida, *Phys. Rev. A* **60**, 3313 (1999).
26. A. A. Svidzinsky, A. L. Fetter, *Phys. Rev. Lett.* **84**, 5919 (2000).
27. F. Dalfovo, S. Giorgini, M. Guilleumas, L. P. Pitaevskii, S. Stringari, *Phys. Rev. A* **56**, 3840 (1997).
28. F. Dalfovo, S. Stringari, *Phys. Rev. A* **63**, 011601 (2001).
29. J. R. Anglin, personal communication.
30. C. Raman *et al.*, *Phys. Rev. Lett.* **83**, 2502 (1999).
31. R. J. Donnelly, *Quantized Vortices in Helium II* (Cambridge Univ. Press, Cambridge, 1991).
32. G. Blatter, M. V. Feigel'man, V. B. Geshkenbein, A. I. Larkin, V. M. Vinokur, *Rev. Mod. Phys.* **66**, 1125 (1994).
33. V. K. Tkachenko, *J. Exp. Theor. Phys.* **23**, 1049 (1966) [*Zh. Eksp. Teor. Fiz.* **50**, 1573 (1966)].
34. S. J. Tsakadze, *Fiz. Nizk. Temp.* **4**, 148 (1978) [*Sov. J. Low Temp. Phys.* **4**, 72 (1978)].



35. We thank J. R. Anglin, A. Görlitz, R. Onofrio, and L. Levitov for useful discussions and critical readings of the manuscript and T. Rosenband for assistance with the two-axis deflector. Supported by NSF, Office of Naval Research, Army Research Office, NASA, and the David and Lucile Packard Foundation.

26 February 2001; accepted 14 March 2001
Published online 22 March 2001;
10.1126/science.1060182
Include this information when citing this paper.


# Self-Assembly of Subnanometer-Diameter Single-Wall $MoS_2$ Nanotubes


**Maja Remskar,[1]* Ales Mrzel,[1] Zora Skraba,[1] Adolf Jesih,[1] Miran Ceh,[1] Jure Demšar,[1] Pierre Stadelmann,[2] Francis Lévy,[3] Dragan Mihailovic[1]**



**We report on the synthesis, structure, and self-assembly of single-wall subnanometer-diameter molybdenum disulfide tubes. The nanotubes are up to hundreds of micrometers long and display diverse self-assembly properties on different length scales, ranging from twisted bundles to regularly shaped "furry" forms. The bundles, which contain interstitial iodine, can be readily disassembled into individual molybdenum disulfide nanotubes. The synthesis was performed using a novel type of catalyzed transport reaction including $C_{60}$ as a growth promoter.**


The discovery of free-standing microscopic one-dimensional molecular structures, such as nanotubes of carbon, has attracted a great deal of attention in the last decade because of various interesting properties associated with their small dimensions, high anisotropy, and intriguing tube-like structures. These range from a variety of quantum effects (*1, 2*) to potentially useful properties such as efficient field emission (*3*) and exceptional mechanical strength (*4*). Finding that curled-up dichalcogenide sheets can also form tube-like objects and fullerene-like nanoparticles (*5–8*) suggested that synthesis of nanotubes made of atoms other than carbon may be possible, and relatively small, 15-nm-diameter tubes made of tungsten and molybdenum disulfide have since been reported (*9–11*). The ultralow friction and wear properties of $MoS_2$ fullerene-like particles (*12, 13*) make inorganic fullerenes important tribological materials. Other layered materials synthesized as nanotubes, tube-like forms, or onion-like structures have been reported, such as boron nitride nanotubes with diameters of a few nanometers (*14, 15*), $W_{18}O_{49}$ hollow microfibers (*16*), and $NiCl_2$ multiwall nanotubes (*17*). Other layered compounds, such as $NbS_2$ (*18*) and GaSe (*19*), have been the subject of extensive theoretical calculations, which have predicted conditions for their stability in cylindrical form and some interesting electronic properties.

We report on the synthesis and basic structural properties of subnanometer-diameter monomolecular $MoS_2$ single-wall nanotubes (SWNTs) produced by a catalyzed transport reaction involving $C_{60}$, and show that the $MoS_2$ nanotubes grow in twisted chiral bundles of identically structured molecules stuck together with interstitial iodine. The tubes vary only in length, but not in diameter.

The single-wall $MoS_2$ nanotubes were grown by a catalyzed transport method using $C_{60}$ as a growth promoter in the reaction. The $C_{60}$ (5 weight %) was added to $MoS_2$ powder in the transport tube as catalyst, and the reaction was run typically for 22 days at 1010 K in an evacuated silica ampoule at a pressure of $10^{-3}$ Pa with a temperature gradient of 6 K/cm. Iodine was used as a transport agent. Approximately 15% (by weight) of the starting material was transported by the reaction to form SWNTs, with the rest remaining in the form of layered material. The transported material was subsequently thoroughly washed with toluene to remove the $C_{60}$.

The transported material grows in the form of bundles oriented perpendicular to the sub-


[1]Jozef Stefan Institute, Jamova 39, SI-1000 Ljubljana, Slovenia. [2]Centre de Microscopie Électronique-CIME, Ecole Polytechnique Fédérale de Lausanne, CH-1015 Lausanne, Switzerland. [3]Institute of Applied Physics, Ecole Polytechnique Fédérale de Lausanne, CH-1015 Lausanne, Switzerland.

*To whom correspondence should be addressed. E-mail: maja.remskar@ijs.si